

Georgia Southern University

## Georgia Southern Commons

---

Department of Manufacturing Engineering  
Faculty Research and Publications

Department of Manufacturing Engineering

---

2017

### Influence of Small Particles Inclusion on Selective Laser Melting of Ti-6Al-4V Powder

Haijun Gong

Georgia Southern University, hgong@georgiasouthern.edu

J. J.S. Dilip

University of Louisville

Li Yang

University of Louisville

Chong Teng

3DSIM LLC

Brent Stucker

3DSIM LLC

Follow this and additional works at: <https://digitalcommons.georgiasouthern.edu/manufact-eng-facpubs>



Part of the [Engineering Commons](#)

---

#### Recommended Citation

Gong, Haijun, J. J.S. Dilip, Li Yang, Chong Teng, Brent Stucker. 2017. "Influence of Small Particles Inclusion on Selective Laser Melting of Ti-6Al-4V Powder." *Proceedings of the International Conference on Mechanical, Materials and Manufacturing*, 272: 1-6: IOP Publishing. doi: 10.1088/1757-899X/272/1/012024 source: <https://iopscience.iop.org/article/10.1088/1757-899X/272/1/012024/meta> <https://digitalcommons.georgiasouthern.edu/manufact-eng-facpubs/16>

This contribution to book is brought to you for free and open access by the Department of Manufacturing Engineering at Georgia Southern Commons. It has been accepted for inclusion in Department of Manufacturing Engineering Faculty Research and Publications by an authorized administrator of Georgia Southern Commons. For more information, please contact [digitalcommons@georgiasouthern.edu](mailto:digitalcommons@georgiasouthern.edu).

PAPER • OPEN ACCESS

## Influence of small particles inclusion on selective laser melting of Ti-6Al-4V powder

To cite this article: Haijun Gong *et al* 2017 *IOP Conf. Ser.: Mater. Sci. Eng.* **272** 012024

View the [article online](#) for updates and enhancements.

### Related content

- [Parameter optimization for selective laser melting of TiAl6V4 alloy by CO2 laser](#)  
R M Baitimerov, P A Lykov, L V Radionova et al.
- [Microstructure and tensile properties of Ti-6Al-4V alloys manufactured by selective laser melting with optimized processing parameters](#)  
L Wang, C Ma, J Huang et al.
- [Analysis of morphology and residual porosity in selective laser melting of Fe powders using single track experiments](#)  
I V Shutov, G A Gordeev, E V Kharanzhevskiy et al.



**IOP | ebooks™**

Bringing you innovative digital publishing with leading voices to create your essential collection of books in STEM research.

Start exploring the collection - download the first chapter of every title for free.

# Influence of small particles inclusion on selective laser melting of Ti-6Al-4V powder

Haijun Gong<sup>1, a)</sup>, J J S Dilip<sup>2</sup>, Li Yang<sup>2</sup>, Chong Teng<sup>3</sup> and Brent Stucker<sup>3</sup>

<sup>1</sup>Georgia Southern University, Statesboro, GA 30460, United States

<sup>2</sup>University of Louisville, Louisville, KY 40292, United States

<sup>3</sup>3DSIM LLC, Park City, UT 84098, United States

<sup>a)</sup>Corresponding author: hgong@georgiasouthern.edu

**Abstract.** The particle size distribution and powder morphology of metallic powders have an important effect on powder bed fusion based additive manufacturing processes, such as selective laser melting (SLM). The process development and parameter optimization require a fundamental understanding of the influence of powder on SLM. This study introduces a pre-alloyed titanium alloy Ti-6Al-4V powder, which has a certain amount of small particles, for SLM. The influence of small particle inclusion is investigated through microscopy of surface topography, elemental and microstructural analysis, and mechanical testing, compared to the Ti-6Al-4V powder provided by SLM machine vendor. It is found that the small particles inclusion in Ti-6Al-4V powder has a noticeable effect on extra laser energy absorption, which may develop imperfections and deteriorate the SLM fatigue performance.

## 1. Introduction

Powder-bed-fusion based Additive Manufacturing (AM) processes, such as selective laser melting (SLM), are increasingly employed for fabricating metal parts. In particular, the SLM titanium alloy parts (e.g. Ti-6Al-4V) are of great interest for aerospace, biomedical and industrial applications due to its geometry complexity, fracture resistance, fatigue behavior, corrosion resistance and biocompatibility [1]. A number of studies have been conducted to characterize the on the mechanical properties of SLM Ti-6Al-4V alloy. For example, Facchini et al. [2] and Ramosoou et al. [3] characterized the microstructure and then tested tensile properties of SLM Ti-6Al-4V parts. Wycisk et al. [4] and Rafi et al. [5] carried out fatigue tests to evaluate the performance of as-built SLM Ti-6Al-4V parts under a high frequency periodical load cycles. Moreover, studies were also carried out on the applications of SLM Ti-6Al-4V parts in industry, aerospace, and medical implants. Caiazzo et al. [6] experimentally studies the use of SLM for manufacturing aircraft components. Cardaropoli et al. [7] discussed the feasibility of producing dental implants through SLM using Ti-6Al-4V pre-alloy powder.

SLM process selectively melts metallic powder layer by layer based upon a sliced CAD file to build a part on a base plate. Inside the SLM building chamber, a recoating unit is used to feed new powder over



the build platform, as shown in figure 1. The widely usage of SLM parts attracts more metallic powder manufacturers to set foot into AM market. Many powder vendors provide metallic powders to SLM equipment users for research and process development. Whether a powder is applicable for SLM process to produce comparable parts is uncertain to the SLM user community. In order to clarify these uncertainties, this study attempts to employ a new Ti-6Al-4V powder (AP&C Inc, Canada) into a commercialized SLM equipment (EOS M270). The powder morphology and particle size distribution were analyzed and compared to a mature Ti-6Al-4V powder (machine vendor provided). Experiments were carried out to develop the optimum process parameters for fully dense parts. Metallography and elemental composition of as-built part was studied. Tensile and fatigue tests were also conducted.

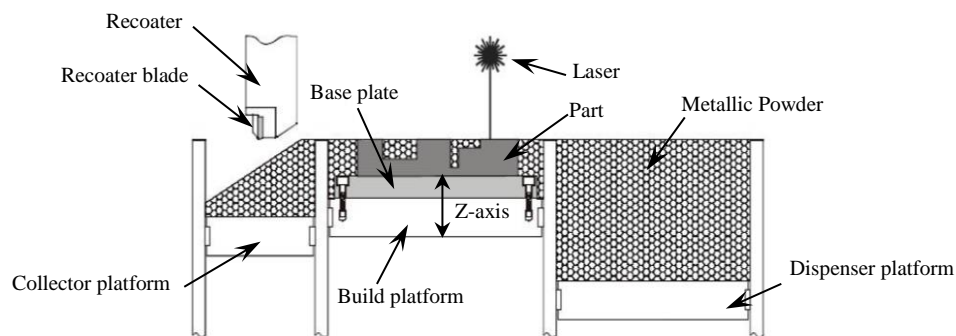


**Figure 1.** Schematic of SLM Process

## 2. Powder Characterization

Figure 2(a) shows the scanning electron microscopy (SEM) of AP&C Ti-6Al-4V powder morphology. It is noted that the AP&C powder particles have the similar spherical shape, compared to the EOS provided Ti-6Al-4V powder (figure 2(b)). A certain amount of fine particles are observable. This is confirmed by the particle size analysis (PSA) using a Microtrac S3000 particle analyzer, as shown in figure 3. The PSA of AP&C powder indicates a size distribution between 17.36  $\mu\text{m}$  ( $D_{10}$ ) and 44.31  $\mu\text{m}$  ( $D_{90}$ ) with Mean Volume (MV) diameter around 30  $\mu\text{m}$ .

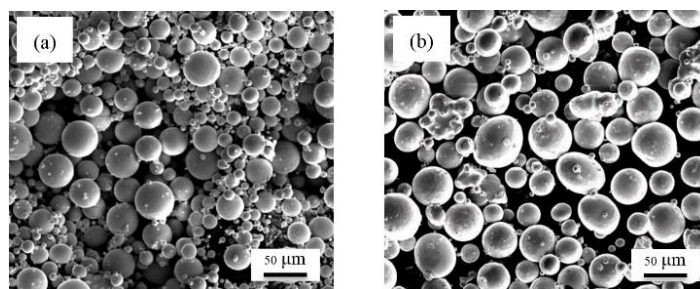


**Figure 2.** SEM of (a) AP&C Ti-6Al-4V Powder and (b) EOS Ti-6Al-4V Powder.

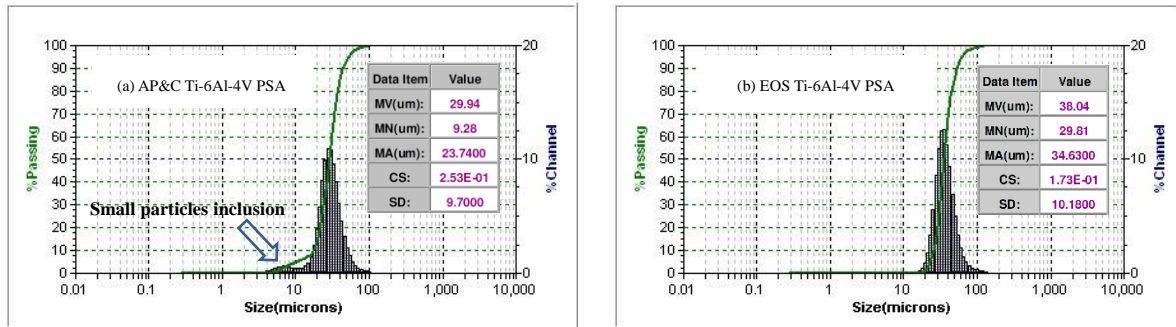


**Figure 3.** Particle Size Distribution of (a) AP&C Ti-6Al-4V and (b) EOS Provided Ti-6Al-4V Powder

### 3. Preliminary Test

AP&C Ti-6Al-4V powder was directly loaded into an EOS M270 for a preliminary test, in order to verify the powder adaptability. The machine has a fiber laser (max 200 W). Galvo mirrors and flat field lens are used to conduct laser beam and maintain a constant focal spot size ( $\sim 100 \mu\text{m}$ ), with scan speed up to 7000 mm/s. Following a standard operation procedure, AP&C powder was melted using the factory default process parameters to fabricate trial parts. After completion, a measurement showed that trial parts have a comparable density to the part fabricated by EOS powder. For further evaluation, microscopy was used to observe the top surface of trial part. As shown in figure 4(a), scan tracks are incoherent on the top surface, deducing voids with small entrapped powder particles inside. So the rough surface for every layer may be expected. The voids could be filled by recoating powder of following layers and melted to minimize porosity inclusion. But there is no apparent evidence that voids could be completely eliminated. A consistent surface topography is desired for using the AP&C powder in SLM process. Thus, development of optimum process parameters for AP&C Ti64 powder is required.

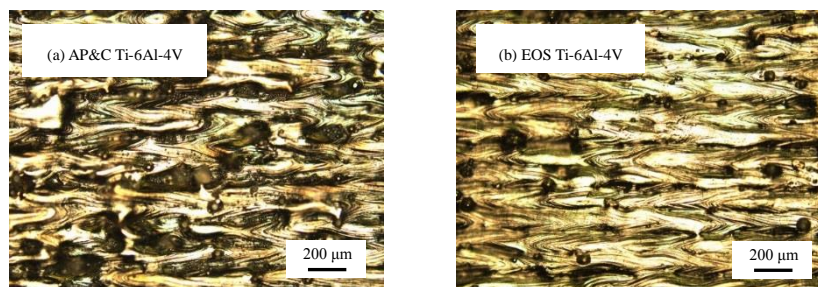


**Figure 4.** Top surface topography of (a) AP&C Ti-6Al-4V sample and (b) EOS Ti-6Al-4V sample.

### 4. Experiment Methods

A factorial design of experiment (DOE) is conducted for investigating the optimum parameters of AP&C powder in the EOS M270 machine to make fully dense parts. The laser power and scan speed have a critical impact on the energy density [8]. Thus, these two parameters were varied, as shown in Table 1, with constant hatch spacing ( $100 \mu\text{m}$ ) and layer thickness ( $30 \mu\text{m}$ ).

**Table 1.** Factors and levels of factorial DOE of AP&C Ti-6Al-4V Powder.

Factor	Level
Laser Power (W)	40, 80, 120, 160
Scan Speed (mm/s)	120, 240, 360, ..., 1560

After samples were fabricated, each specimen's density was measured using the Archimedes method (ASTM B962-08) [9] to estimate porosity and determine optimum parameters. As-built parts were sectioned, abrasively grinded and polished, and etched for metallography. It is found that the laser power 120 W and scan speed 960 mm/s are eligible to produce fully dense parts, in conjunction with other default process parameters. Cylindrical bars were built in the Z orientation (ISO/ASTM 52921, 2013) using this optimum parameter set, and then machined to specimens conforming to ASTM E8 for tensile testing and ASTM E466 for fatigue testing. Tensile tests were carried out using an Instron 5569A tensile testing machine. High cycle fatigue tests were performed on a 10kN Instron Electropulse 10000 fatigue testing machine. Sinusoidal load was applied to fatigue specimens axially (50 Hz, stress ratio  $R=0.1$ ). Fatigue testing was stopped when the specimens broke or the fatigue cycles reached  $10^7$  cycles. Fracture surface was examined by a FEI Nova NanoSEM 600 SEM.

## 5. Results and Discussion

### 5.1 Microstructural Analysis

Microstructural evolution is primarily a function of cooling rate. The SLM process undergoes a very high cooling rate which results in a lenticular martensitic ( $\alpha'$ ) microstructure of Ti-6Al-4V, as shown in figure 5. The martensitic phase of AP&C Ti-6Al-4V sample shows similar microscopic morphology in comparison with EOS Ti-6Al-4V sample. Martensitic laths originated from the prior  $\beta$  grain boundaries. All  $\beta$  phases (BCC) are transformed to hexagonal martensite. The microstructure indicates that the small particles inclusion does not influence the formation of crystalline structures in the SLM process.

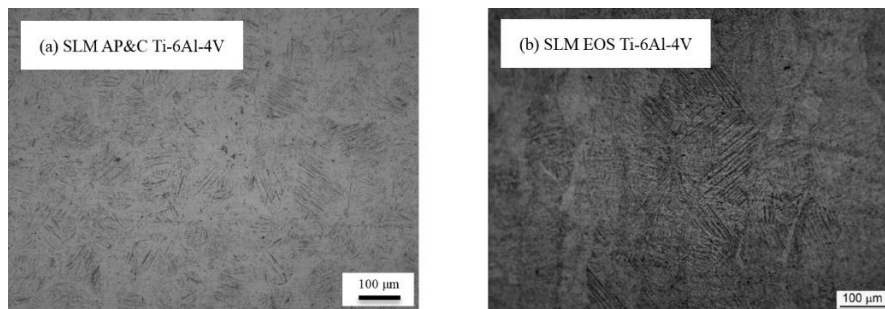


**Figure 5.** Optical microscopy of microstructure of SLM samples

### 5.2 Composition Analysis

The chemical composition of SLM samples was analyzed using energy dispersive X-ray analysis (EDAX). The EDAX is a commonly used analytical technique for the elemental analysis, which allows a unique set of peaks on its electromagnetic emission spectrum for each element. The EDAX spectrum of AP&C sample and EOS sample are shown in figure 6.

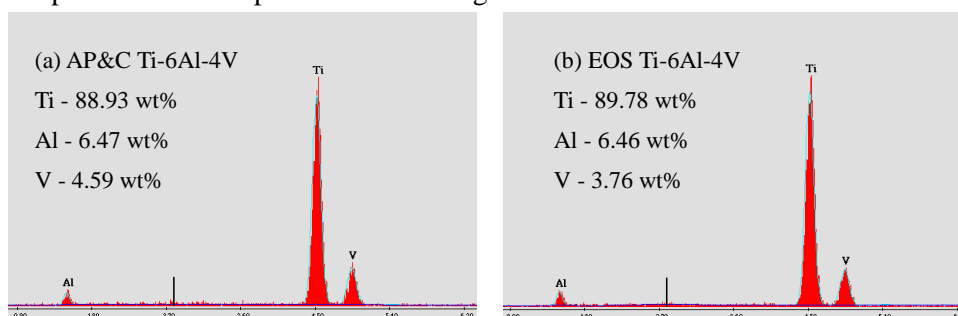


**Figure 6.** EDAX spectrum of (a) AP&C Ti-6Al-4V sample and (b) EOS Ti-6Al-4V sample.

There is no apparent difference in the composition between Ti-6Al-4V samples. The chemical composition is primarily determined by the composition of pre-alloyed Ti-6Al-4V powder. The melting and solidification process of SLM have few influence on the elemental composition. The variation of particle size distribution could have an impact on the mass transportation during the laser melting process. The small particles may be more easily ejected owing to the recoil force of metallic vapor. But the chemical composition of Ti-6Al-4V sample is not influenced.

### 5.3 Tensile Property

Six duplicate specimens were performed for the tensile test. Corresponding tensile stress-strain curves were obtained directly from the Instron system, as shown in figure 7. Tensile properties are summarized in Table 2, in comparison with EOS Ti-6Al-4V. Generally, the material properties of AP&C specimens and EOS specimens are comparable. Both SLM Ti-6Al-4V materials show a higher yield strength and tensile strength compared to the wrought Ti-6Al-4V samples, due to the observed martensitic microstructure. The martensite grains nucleate and grow at a rapid rate, resulting in a very small grain size (a greater total grain boundary area). The grain boundaries impede the slip process and increase the strength of the material. No significant influence of small particles inclusion is observed on the tensile property.

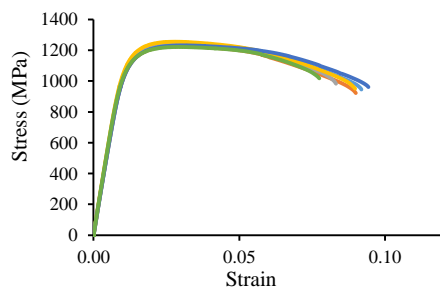


**Figure 7.** Stress-strain curve of SLM AP&C Ti-6Al-4V samples.

**Table 2.** Tensile Properties of SLM Ti-6Al-4V samples.

	SLM AP&C Ti-6Al-4V	SLM EOS Ti-6Al-4V <sup>a</sup>
Yield Strength (MPa)	1098 ± 45	1150 ± 80
UTS (MPa)	1237 ± 39	1290 ± 80
Strain at Break (%)	8.8 ± 1.8	8 ± 4
Young's Modulus (GPa)	109 ± 6.3	110 ± 5

<sup>a</sup> www.eos.info

### 5.4 Fatigue Performance

As for the high-cycle fatigue test, materials performance is shown in figure 8(a), comparing AP&C and EOS specimens. It is noted that the AP&C specimens show considerable scatter in fatigue life. The fatigue limit is also lower than the EOS specimens, which was reported by Rafi et al [5]. The AP&C specimens appear to have an inferior fatigue behavior, as opposed to the tensile properties. Although it is hard to assert that the inclusion of small particles deteriorate the fatigue performance, the variation of powder and process parameters undoubtedly have an influence on the Ti-6Al-4V parts. The small particles inclusion may play a critical role during the SLM process. Due to the small particles inclusion, the absorption is greatly increased on powder content resulted by the multiple scattering of laser [10]. A higher temperature and larger melt pool size can be expected. The drastic phase transformation may cause an unsteady melt pool and scan tracks. Keyhole defects, volumetric voids, and impurities have a great potential to be included in the SLM specimens. The fatigue behavior is sensitive to these imperfections, especially when a high frequency cyclic load is applied. The fractography in figure 8(b) shows the crack initiation site on the fracture surface of an AP&C fatigue specimen. It can be clearly seen that small particles are entrapped in a defective site, which cause stress concentration.

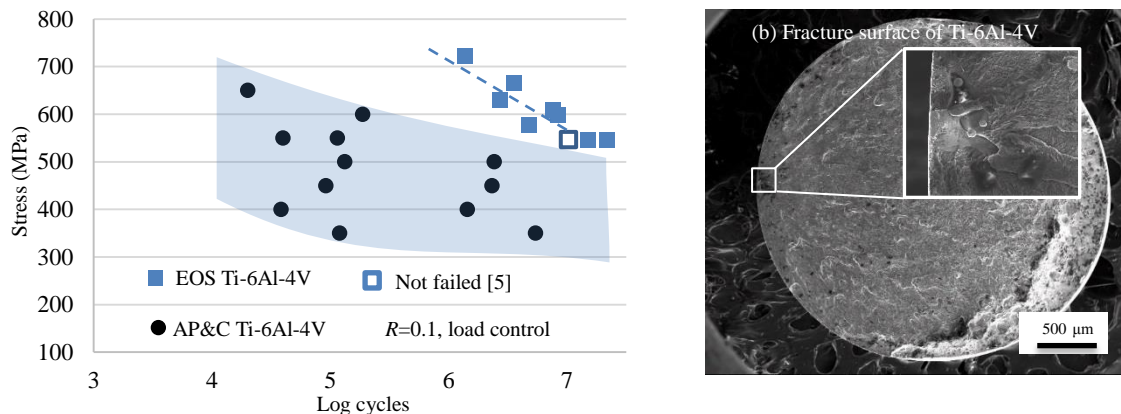


**Figure 8.** SLM Ti-6Al-4V fatigue specimens (a) *S-N* curve and (b) fractography.

## 6. Conclusion

This study introduces a new Ti-6Al-4V powder for SLM process. The influence of small particles inclusion is investigated. It is found that process parameters need to be tuned for fabricating fully dense parts if using new powder. The small particle inclusion does not influence the microstructure and elemental composition of SLM Ti-6Al-4V parts. The tensile property of AP&C Ti-6Al-4V specimens is also comparable to the specimen fabricated by EOS powder. However, the fatigue performance of AP&C specimens is poor. The small particles inclusion may influence the laser absorption on the powder bed, resulting in imperfections in the SLM material. Thus, future research is highly desired to conduct quantitative analysis of small particles in the powder system.

## 7. Reference

- [1] Soboyejo W O and Srivatsan T S 2006 *Advanced Structural Materials: Properties, Design Optimization, and Applications* (Boca Raton: CRC Press) p 359-400
- [2] Facchini L, Magalini E, Robotti P, Molinari A, Höges S and Wissenbach K 2010 *Rapid Prototyping J.* **16** 450-9
- [3] Ramosoou M K E, Booyesen G and Ngonda T N 2011 *Proc. Materials Science and Technology Conference (MS&T)* (Materials Park: ASM International) p 1460-8
- [4] Wycisk E, Emmelmann C, Siddique S and Walther F 2013 *Adv. Mater. Res.* **816-817** 134-9
- [5] Rafi K, Karthik N V, Gong H, Starr T and Stucker B 2013 *J. Mater. Eng. Perform.* **22** 3872-83
- [6] Caiazzo F, Cardaropoli F, Alfieri V, Sergi V and Cuccaro L 2013 *Proc. of SPIE* 8677
- [7] Cardaropoli F, Alfieri V, Caiazzo F and Sergi V 2012 *Adv. Mater. Res.* **535-537**, 1222-9
- [8] Thijs L, Verhaeghe F, Craeghs T, Van Humbeeck J and Kruth J P 2010 *Acta Materialia* **58**, 3303-12
- [9] Spierings A B and Schneider M 2011 *Rapid Prototyping J.* **17**, 380-6
- [10] Boley C D, Khairallah S A and Rubenchik A M 2015 *Applied Optics* **54**, 2477-82